

- (7) (a) H. C. Gardner and J. K. Kochi, *J. Am. Chem. Soc.*, **97**, 1855 (1975); (b) *ibid.*, **96**, 1982 (1974).
- (8) (a) S. R. Su and A. Wojcicki, *Inorg. Chem.*, **14**, 89 (1975); J. A. Hanna and A. Wojcicki, *Inorg. Chim. Acta*, **9**, 55 (1974); cf. M. R. Churchill and S. W.-Y. Chang, *Inorg. Chem.*, **14**, 98 (1975); (b) N. Chaudhury, M. G. Kekre, and R. J. Puddephatt, *J. Organomet. Chem.*, **73**, C17 (1974).
- (9) (a) H. C. Gardner and J. K. Kochi, *J. Am. Chem. Soc.*, **97**, 5026 (1975); (b) *ibid.*, **98**, 558 (1976).
- (10) The existence of weak or experimentally contact interactions as defined by Orgel and Mulliken is inferred in the alkylmetal-TCNE systems. Compare L. E. Orgel and R. S. Mulliken, *J. Am. Chem. Soc.*, **79**, 4838 (1957); P. R. Hammond, *J. Chem. Soc. A*, 3025 (1971); P. R. Hammond and L. A. Burkhardt, *J. Phys. Chem.*, **74**, 639 (1970). The question as to whether the charge transfer absorption is due to 1:1 complexes or pairs of contiguous molecules is left open.
- (11) Linear plots were obtained. However, the intercepts for determining  $K$ , the "formation constant", and  $\epsilon$ , the extinction coefficient of the complex at  $\lambda_{\text{max}}$  (CT), were very near zero and indicated that the complexes are weak.
- (12) W. J. Middleton, E. L. Little, D. D. Coffman, and V. A. Englehardt, *J. Am. Chem. Soc.*, **80**, 2795 (1958).
- (13) O. W. Webster, W. Mahler, and R. E. Benson, *J. Am. Chem. Soc.*, **84**, 3678 (1962).
- (14) (a) E. M. Kosower, "Physical Organic Chemistry", Wiley, New York, N.Y., 1968, p 293 ff; (b) N. S. Isaacs, *J. Chem. Soc. B*, 1053 (1966).
- (15) A. G. Davies and R. J. Puddephatt, *J. Chem. Soc. C*, 2663 (1967).
- (16) The metastability of trialkyllead and -tin salts of strong acids prevents their isolation in pure form. To isolate the anions, the cationic species were first removed by precipitation with *N,N*-diethyldithiocarbamate salts followed by treatment of the filtrate with tetramethylammonium chloride.<sup>9</sup>
- (17) The data in ref 6a were incorrectly plotted. The data are correctly plotted in Figure 3 of this paper.
- (18) (a) R. S. Mulliken and W. B. Person, "Molecular Complexes, a Lecture and Reprint Volume", Wiley, New York, N.Y., 1969; (b) ref 4, Chapter 7.
- (19) A more general representation includes charge transfer contributions in the ground state and no bond interactions in the excited state.
- (20) For a discussion of the stabilities of organometallic cation-radicals see ref 3 and 23.
- (21) J. K. Kochi, D. G. Morrell, and I. H. Elson, *J. Organomet. Chem.*, **84**, C7 (1975).
- (22) (a) N. A. Clinton and J. K. Kochi, *J. Organomet. Chem.*, **56**, 243 (1973); (b) B. G. Hobrock and R. W. Kiser, *J. Phys. Chem.*, **65**, 2186 (1961); (c) American Petroleum Institute, research project 44, Carnegie Institute of Technology, Pittsburgh, Pa., mass spectrum no. 700; (d) M. F. Lappert, J. B. Pedley, J. Simpson, and T. R. Spalding, *J. Organomet. Chem.*, **29**, 195 (1971).
- (23) (a) A. D. Baker, D. Betteridge, N. R. Kemp, and R. E. Kirby, *Anal. Chem.*, **43**, 375 (1971); B. J. Cocksey, J. H. D. Eland, and C. J. Danby, *J. Chem. Soc. B*, 790 (1971); (b) V. F. Traven and R. West, *J. Gen. Chem. USSR*, **44**, 1803 (1974); (c) J. H. D. Eland, *Int. J. Mass Spectrom. Ion Phys.*, **4**, 37 (1970); (d) H. Bock and W. Ensslin, *Angew. Chem., Int. Ed. Engl.*, **10**, 404 (1970).
- (24) E. M. Kosower, *Prog. Phys. Org. Chem.*, **3**, 81 (1965). The curves are drawn so that the intermolecular distances in the ion pair is less than that in the unchanged complex.
- (25) There is some evidence among mercury derivatives of **6** for rearrangement to **7** (see experimental section).
- (26) (a) Cf. J. Halpern, R. J. Legare, and R. Lumry, *J. Am. Chem. Soc.*, **85**, 680 (1963); (b) J. Halpern and M. Pribanlc, *ibid.*, **90**, 5942 (1968); (c) P. Abley and J. Halpern, *Chem. Commun.*, 1238 (1971); (d) A. G. Sykes and R. F. Thorneley, *J. Chem. Soc. A*, 232 (1970).
- (27) N. A. Clinton, H. C. Gardner, and J. K. Kochi, *J. Organomet. Chem.*, **56**, 227 (1973).
- (28) O. W. Webster, W. Mahler, and R. E. Benson, *J. Am. Chem. Soc.*, **84**, 3678 (1962).
- (29) W. D. Phillips, J. C. Rowell, and S. I. Weissman, *J. Chem. Phys.*, **33**, 626 (1960).
- (30) It should be emphasized that spectral observations by themselves do not establish the direct involvement of TCNE<sup>-</sup> in the insertion pathway.
- (31) Unlike the TCNE insertion reaction, a clear distinction can be readily made between transfer of R<sup>-</sup> or R<sup>+</sup> from alkyllead species during oxidative cleavages with hexachloroiridate(VI).
- (32) P. J. Krusic, H. Stoklosa, L. E. Manzer, and P. Meakin, *J. Am. Chem. Soc.*, **97**, 667 (1975).
- (33) This qualitative analysis assumes that the rates of reactions 22 and 23 are not highly sensitive to R.
- (34) N. A. Clinton and J. K. Kochi, *J. Organomet. Chem.*, **42**, 229 (1972).
- (35) (a) G. Calingaert, H. Soroos, and H. Shapiro, *J. Am. Chem. Soc.*, **62**, 1104 (1940); (b) G. Calingaert, F. J. Dykstra, and H. Shapiro, *ibid.*, **67**, 190 (1945); (c) H. Shapiro and F. W. Frey, "The Organic Compounds of Lead", Wiley, New York, N.Y., 1968, Chapter XI.
- (36) F. Huber, H. Horn, and H. J. Haupt, *Z. Naturforsch. B*, **22**, 918 (1967).
- (37) The relevant NMR spectra are included in the Ph.D. dissertation of H. C. Gardner, Indiana University, 1975.
- (38) L. C. Willemsens and G. J. M. Van der Kerk, "Investigations in the Field of Organolead Chemistry", *Int. Lead Zinc Res. Org.*, 1965, p 69.
- (39) Cf. V. S. Petrosyan and O. A. Reutov, *J. Organomet. Chem.*, **76**, 123 (1974), for a summary of NMR parameters for organomercurials.
- (40) H. Gilman and R. E. Brown, *J. Am. Chem. Soc.*, **52**, 3314 (1930).
- (41) Cf. P. T. Narasimham and M. T. Rogers, *J. Chem. Phys.*, **34**, 1049 (1961).
- (42) J. Lorberth and H. Varenkamp, *J. Organomet. Chem.*, **11**, 111 (1968).

## Thin Layer Spectroelectrochemical Study of Vitamin B<sub>12</sub> and Related Cobalamin Compounds in Aqueous Media

Thomas M. Kenyhercz, Thomas P. DeAngelis, Barbara J. Norris,  
William R. Heineman, and Harry B. Mark, Jr.\*

Contribution from the Department of Chemistry, University of Cincinnati,  
Cincinnati, Ohio 45221. Received September 8, 1975

**Abstract:** The oxidation-reduction behavior of vitamin B<sub>12</sub> and related cobalamins in aqueous media has been studied by a spectroelectrochemical technique using an optically transparent thin layer electrode cell (OTTLE). It was found, contrary to previous reports, that all of the cobalamins are reduced via two distinct one-electron steps. The rate of the electron transfer in the first one-electron step is unusually slow in all cases except for aquocob(III)alamin, B<sub>12a</sub>, and no wave is observed even at the slow voltage scan rates used in polarography. It is also shown that aquocob(III)alamin, previously assumed to be a single compound, is a nonequilibrium mixture of two compounds which have an approximately 500 mV difference in the one-electron reduction potential. It is suggested that the two species may be a "base on" and "base off" form with respect to the corrin ring side chain benzimidazole in the y-axial position.

The electrochemical behavior of vitamin B<sub>12</sub> (cyanocob(III)alamin) and related cobalamin compounds in aqueous media is of importance for elucidating the biomechanistic reaction sequences which involve cobalamin species.<sup>1</sup> There has been considerable study of the redox processes of cobalamins using the conventional electroanalytical techniques of polarography,<sup>2-14</sup> coulometry,<sup>9,15,16</sup> and cyclic voltammetry,<sup>17-20</sup> and diverse working electrode materials

such as mercury<sup>2-20</sup> and platinum.<sup>12,20</sup> However, the interpretation of the electrochemical data to unambiguously determine even the most fundamental parameters such as the thermodynamic redox potentials, the number of electrons ( $n$  values) involved in the electron transfer steps, and the sequence of steps in the mechanism has not been possible because of numerous complicating conditions. The complications encompass strong adsorption of both reactant and

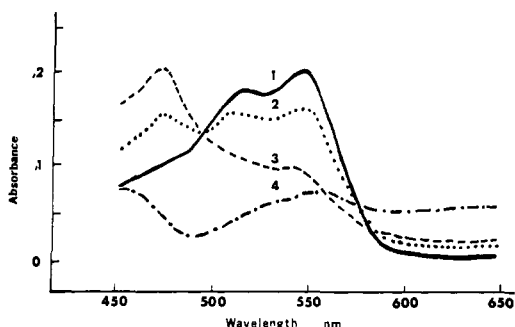


**Figure 1.** Spectropotentiostatic curves for the reduction of  $B_{12}$  at various applied potentials vs. SCE in a Hg-Ni OTTLE: (1)  $B_{12}$  potentiostated at 0.000 V vs. SCE; (2)  $B_{12}$  potentiostated at -0.600 V vs. SCE; (3)  $B_{12}$  potentiostated at -0.660 V vs. SCE; (4)  $B_{12}$  potentiostated at -1.000 V vs. SCE.

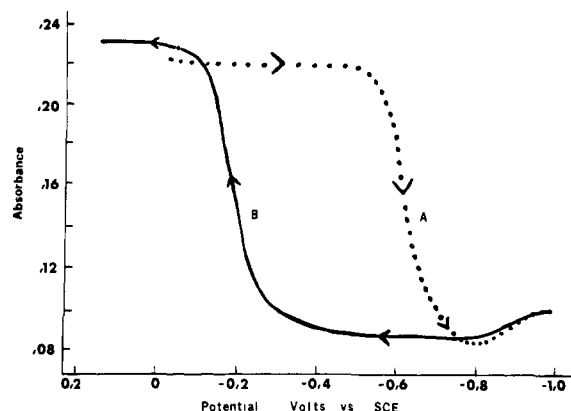


**Figure 2.** Potential-absorbance curves for the reduction (curve A) and oxidation (curve B) of 1.2 mM  $B_{12}$  monitored at 550 nm: 1.0 M  $Na_2SO_4$ ; 0.1 M  $NaNO_3$ ; pH 7.0; Hg-Ni minigrid; cell thickness, 0.017 cm.

product, irreversibility of the redox reactions, unusual medium effects involving the solvent system and the supporting electrolyte, and marked variation of electrode kinetics with the electrode material.<sup>2-20</sup> Recently, new techniques employing minigrid electrodes in conjunction with thin layer electrolysis cells<sup>21</sup> have been developed which have proved useful to the study of the basic redox properties of cytochrome *c*.<sup>22</sup> This paper reports the results obtained by using thin layer minigrid electrode cells to study the electrochemical and spectroelectrochemical behavior of cyanocobalamin ( $B_{12}$ ), aquocobalamin ( $B_{12a}$ ), and dicyanocobalamin ( $B_{12-CN}$ ).

### Experimental Section

The electrochemical instrumentation was of conventional operational amplifier design.<sup>22</sup> A Houston Instruments Model 2000 X-Y recorder was used to output the electrochemical data and a Cary 14 spectrophotometer was employed to monitor optical changes during the course of spectroelectrochemical experiments.<sup>22</sup> Digitec 261 and Fluke 8000A digital voltmeters were employed to monitor applied potential and final current levels in the spectropotentiostatic experiments. In the experiments, the optically transparent thin layer electrode (OTTLE) which served as the working electrode was constructed according to established procedures using either nickel (333 lines/in., 57% transmittance) or gold (500 lines/in., 60% transmittance) minigrids (Buckbee Mears Co., St. Paul, Minn.), microscope slides ( $1 \times 3$  in.) and 2 mil Fluorofilm DF-1200 tape (Dilectrix Corp., Farmingdale, N.Y.).<sup>22</sup> The preparation of the mercury coated nickel minigrid electrode used herein has been described previously.<sup>23</sup> The exact thickness of each cell was spectrophotometrically calibrated using standard solutions of 2,6-dichlorophenolindophenol or vitamin  $B_{12-CN}$ . An average cell thickness of 0.017 cm was obtained. The three-electrode system also employed a platinum wire as the auxiliary electrode while a miniature SCE served as the reference electrode.<sup>23</sup> Exhaustive

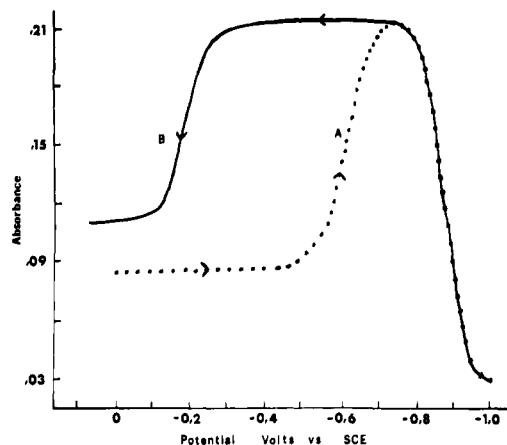


**Figure 3.** Potential-absorbance curves for the reduction (curve A) and oxidation (curve B) of 1.2 mM  $B_{12}$  monitored at 475 nm: 1.0 M  $Na_2SO_4$ ; 0.1 M  $NaNO_3$ ; pH 7.0; Hg-Ni minigrid; cell thickness, 0.017 cm.

coulometry and cyclic voltammetry were performed on the cobalamin systems. The spectroelectrochemical experiments were carried out in the presence and absence of the electron transfer mediator, 2,6-dichlorophenolindophenol (Fluka, Columbia Organic Chemicals, Columbia, S.C.) in an effort to determine thermodynamic redox potentials of the various cobalamins and to crosscheck the thin layer electrochemical information.<sup>22</sup> Crystalline cyanocobalamin, vitamin  $B_{12}$  (Sigma Chemical Co., St. Louis, Mo.), was used without further purification and was used in the synthesis of aquocobalamin ( $B_{12a}$ )<sup>13</sup> and dicyanocobalamin ( $B_{12-CN}$ ).<sup>11</sup> Alternately,  $B_{12}$  samples from Nutritional Biochemical were used in conjunction with the potentiostatic reduction method;<sup>13</sup>  $B_{12a}$  was also purchased from Mann Research Laboratory and prepared from  $B_{12}$  by a chemical synthesis involving borohydride reduction of  $B_{12}$ .<sup>24</sup> All solutions were  $1 \times 10^{-3}$  M in the cobalamin species and 1.0 M in  $Na_2SO_4$ <sup>20</sup> and either 0.1 M  $NaNO_3$  or 0.1 M KCN was used as the supporting electrolyte as designated in the text.

### Results and Discussions

**Spectroelectrochemistry of the Cobalamin Systems.** As changes in the valence of cobalt, the central metal ion of the cobalamins, are reflected by distinct changes in the visible absorption spectra, a coupling of electrochemical and spectroscopic measurements was performed to elucidate the redox behavior of the cobalamins. Spectroelectrochemical experiments were carried out using the optically transparent thin layer electrochemical cells (OTTLE) in the presence and absence of the electron transfer mediator, 2,6-dichlorophenolindophenol.<sup>22</sup> The cobalamin-containing OTTLE cells were potentiostated while the optical absorbance of a peak of interest and current levels were monitored. When both the absorbance stopped changing and the current levels had fallen to essentially zero ( $\leq 0.1 \mu A$ ), the spectrum of the solution in the OTTLE cell was recorded. Figure 1 shows how the spectra of a  $B_{12}$  solution varies as the applied potential is changed. Curve 1 of Figure 1 for which the Hg-Ni minigrid electrode was potentiostated at 0.00 V is a typical spectrum for  $B_{12}$  (a cob(III)alamin) with characteristic peaks at 520 and 550 nm.<sup>24</sup> The spectrum obtained by potentiostating at -0.600 V (curve 2, Figure 1) shows that the concentration of the cob(III)alamin is decreasing as seen by the decrease in the 520- and 550-nm peaks and the development of a new peak at 475 nm. This 475-nm peak is typical of that reported for  $B_{12r}$ , a cob(II)alamin species.<sup>25</sup> On potentiostating at -0.660 V, the cobalamin is found to be almost completely converted to  $B_{12r}$  (curve 3, Figure 1). On potentiostating at -1.0 V, the spectrum obtained matches that obtained by other workers<sup>6,24</sup> for  $B_{12s}$ , a cob(I)alamin species with a weakly ab-

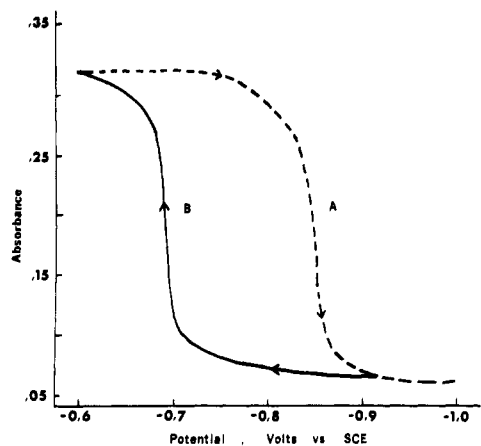


**Figure 4.** Potential-absorbance curves for the reduction (curve A) and oxidation (curve B) of 1.2 mM  $B_{12}$ -CN monitored at 580 nm; 1.0 M  $Na_2SO_4$ ; 0.1 M KCN; pH 10.4; Hg-Ni minigrid; cell thickness, 0.017 cm.

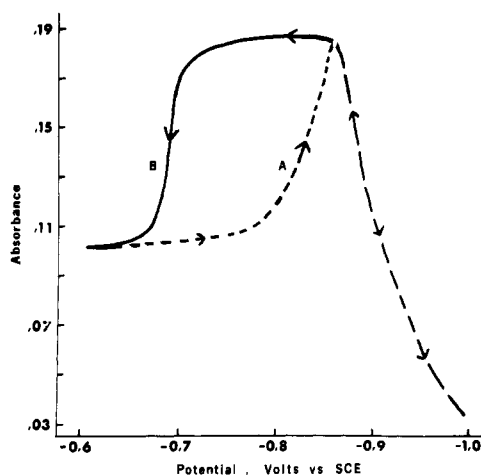


**Figure 5.** Potential-absorbance curves for the reduction (curve A) and oxidation (curve B) of 1.2 mM  $B_{12}$ -CN monitored at 475 nm; 1.0 M  $Na_2SO_4$ ; 0.1 M KCN; pH 10.4; Hg-Ni minigrid; cell thickness, 0.017 cm.

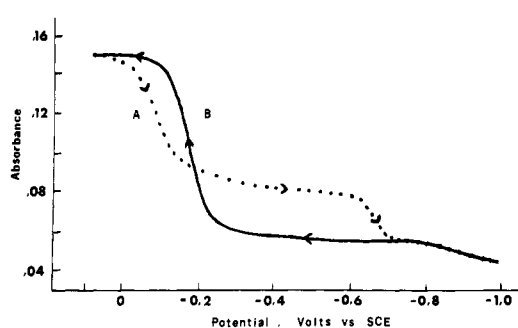


**Figure 6.** Potential-absorbance curves for the reduction (curve A) and oxidation (curve B) of 0.9 mM  $B_{12a}$  monitored at 530 nm; 1.0 M  $Na_2SO_4$ ; 0.1 M  $NaNO_3$ ; pH 7.01; Hg-Ni minigrid; cell thickness, 0.017 cm.

sorbing broad peak at 560 nm and a tapered shoulder in the region of 460 nm.

The quantitative change in the various peak absorbance values as a function of applied potential for  $B_{12}$ ,  $B_{12a}$ , and  $B_{12}$ -CN are shown in Figures 2 through 9. Curve A of Figure 2 shows the effect of potential at a Hg-Ni minigrid electrode on the absorbance of the 550-nm peak of  $B_{12}$  as it is reduced. The  $B_{12}$  is totally reduced to a cob(II)alamin

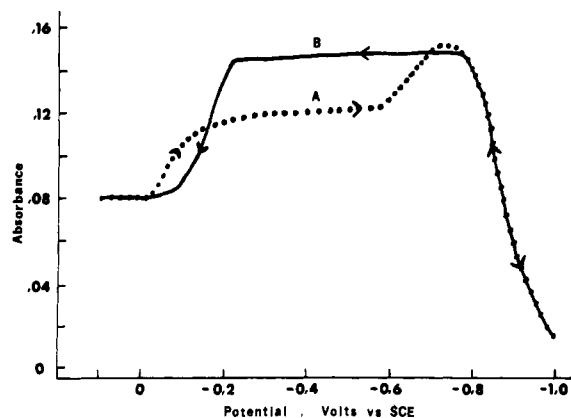


**Figure 7.** Potential-absorbance curves for the reduction (curve A) and oxidation (curve B) of 0.9 mM  $B_{12a}$  monitored at 475 nm; 1.0 M  $Na_2SO_4$ ; 0.1 M  $NaNO_3$ ; pH 7.0; Hg-Ni minigrid. Cell thickness, 0.017 cm.

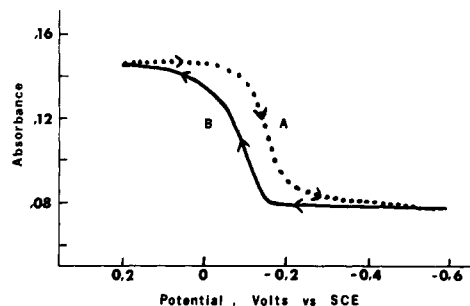


**Figure 8.** Potential-absorbance curves for the reduction (curve A) and oxidation (curve B) of 0.9 mM  $B_{12a}$  monitored at 525 nm; 1.0 M  $Na_2SO_4$ ; 0.1 M  $NaNO_3$ ; pH 7.0; Au minigrid and 2,6-dichlorophenol-indophenol; cell thickness, 0.021 cm.

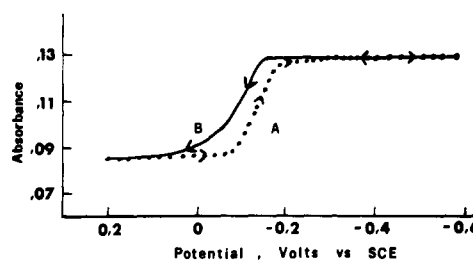


**Figure 9.** Potential-absorbance curves for the reduction (curve A) and oxidation (curve B) of 0.9 mM  $B_{12a}$  monitored at 475 nm; 1.0 M  $Na_2SO_4$ ; 0.1 M  $NaNO_3$ ; pH 7.0; Au minigrid and 2,6-dichlorophenol-indophenol; cell thickness, 0.021 cm.

over a relatively narrow potential range (approximately 200 mV) with an absorbance "half-wave potential" of about  $-0.63$  V. The slight increase in the absorbance between  $-0.8$  and  $-1.0$  V is the result of the further reduction of cob(II)alamin to cob(I)alamin which would be expected, as  $B_{12s}$ , a cob(I)alamin, exhibits a broad peak in the region of 560 nm.<sup>25</sup> The effect of potential on the absorbance at 550 nm for the reoxidation of cyanocob(I)alamin is shown by curve B of Figure 2. The quantitative reoxidation of the cob(I)- to cob(II)alamin occurs over the same potential range ( $-1.0$  to  $-0.8$  V) as shown in Figure 2 and is coincident with the behavior observed in curves A and B of Figure 3 (absorbance vs. potential curves for the 475-nm peak; the cob(II)alamin in the same potential region. However, the reoxidation of the cob(II)alamin to  $B_{12}$  occurs only when the potentials are 400 mV positive to those of the reduction potentials as can be seen from the hysteresis in curves A and B of both Figures 2 and 3 in the  $-0.1$  to  $-0.7$  V range.

A shorter potential scan,  $-1.0$  to  $-0.8$  V, OTTLE experiment with the same conditions as Figure 3 (going only to the cob(II)amin) showed the exact same hysteresis. It is important to note that  $B_{12}$  appears to be completely regenerated as the optical absorbance eventually returns to its initial value (seen in Figure 2). Figure 3, however, appears to be contradictory with respect to the reoxidation part of the above explanation. If the 475-nm peak, corresponding to cob(II)alamin formation, is to be used as an accurate indicator of cob(I)-, cob(II)-, or various cob(III)alamin species being present, then it would seem that in addition to reforming  $B_{12}$ , another cob(III)alamin may also have been formed. Spectral data obtained on the subsequent reduction of the cobalamin formed following the reoxidation of  $B_{12}$  (curve B, Figure 3), indicates a slight rise in the initial portion of the cobalamin absorbance-potential wave (monitored by the development of the 475-nm peak). The magnitude of this absorbance-potential rise remains constant as the cobalamin is recycled potentiostatically. The initial rise does not become an appreciable portion of the  $B_{12}$  absorbance-potential curve during the potentiostatic cycling process, but does resemble the behavior of  $B_{12a}$  shown in curve A of Figure 7.

The same set of experiments was performed for  $B_{12}$ -CN at a Hg-Ni electrode. As can be seen from Figures 4 and 5 dicyanocobalamin behaves quite similarly to  $B_{12}$ , the only difference being the potential region where  $B_{12}$ -CN reoxidation occurs. The hysteresis in the dicyanocobalamin reoxidation is significantly less than for  $B_{12}$  (only about 180 mV difference in the half-absorbance potentials for  $B_{12}$ -CN reduction and reoxidation curves in Figures 4 and 5).

Vitamin  $B_{12a}$  was also investigated at a Hg-Ni electrode in a similar set of experiments. Curves A of Figure 6 (the 530-nm peak) and Figure 7 (the 475-nm peak) show that  $B_{12a}$  undergoes an unusual two-step process, as illustrated by the breaks at about  $-0.06$  and  $-0.65$  V, before complete conversion to a cob(II)alamin species. Curve A of Figures 6 and 7 shows that the cob(II)alamin is then reduced to cob(I)alamin as the potential increases from  $-0.8$  to  $-1.0$  V. On reoxidation, curve B of Figure 7, the cob(I)alamin is reversibly reoxidized to cob(II)alamin over the same potential range as in the negative scan. However, the B curves in both Figures 6 and 7 indicate that the reoxidation which corresponds to a quantitative regeneration of  $B_{12a}$  from the cob(II)alamin species is a single step process which oddly occurs at a potential negative to the first reduction step (ca.  $-50$  mV).

To check the unique spectroelectrochemical properties of  $B_{12a}$ , other samples of  $B_{12a}$  from different sources and preparations were examined, and, also, the electrochemical preparation was recycled a number of times. The spectroelectrochemical behavior at a particular wavelength for  $B_{12a}$  from the various preparations gave spectropotentiostatic curves (OTTLEgrams) identical with those presented herein. Also, spectropotentiostatic cycling of  $B_{12a}$  gave reproducible sets of curves. It is interesting that the absorbance-potential waves for  $B_{12a}$  in the OTTLE experiments do not correspond to any peaks in the cyclic voltammogram of  $B_{12a}$  at the same electrode (see Figure 12). However, the three absorbance-potential "waves" for the reduction of  $B_{12a}$  do correlate reasonably well with the three waves observed in the previously reported polarography of  $B_{12a}$ .<sup>6,7,13</sup> To understand the unusual two-step process in the reduction of  $B_{12a}$  to a cob(II)alamin species and to determine if the electrode itself is playing a role in the electron transfer kinetics, the mediator 2,6-dichlorophenolindophenol was used in conjunction with the Au minigrid electrode.<sup>22</sup> The mediator functions as the primary electron transfer agent between the electrode and a redox system that has very slow

heterogeneous electron transfer rates. Thus, the mediator accelerates the overall electrochemical reaction of the system of interest. The choice of this mediator was determined by the potential region of interest in this case ( $+0.2$  to  $-0.2$  V vs. SCE). The Au minigrid electrode was used to eliminate the possibility of oxidation of the working electrode material in this potential region and because the cyclic voltammograms of  $B_{12a}$  exhibited a more well-defined wave at an intermediate potential, and  $B_{12a}$  appeared to be less strongly adsorbed on the Au electrode. The absorbance changes of the 525-nm ( $B_{12a}$ ) and 475-nm ( $B_{12r}$ ) bands as a function of the applied potential are shown in Figures 8 and 9, respectively. Curve A of Figure 8 shows only one "wave" with a half-absorbance potential of  $-0.15$  V in the  $+0.2$  to  $-0.6$  V potential region scanned. From curve B of Figure 8 it can be seen that the produced  $B_{12r}$  is totally reoxidized to  $B_{12a}$  with little hysteresis (half-absorbance potential of about  $-0.09$  V for the reoxidation) in the process. The changes in the 475-nm absorbance peak (Figure 9) again indicate only one "wave" for the generation and subsequent reoxidation of the  $B_{12r}$  with half-absorbance potentials which correspond favorably to those of the  $B_{12a}$  "waves" in Figure 8. Thus, the mediator-Au electrode system reflects a more typical redox behavior as it eliminates the unusual hysteresis effect where the reoxidation of  $B_{12a}$  from  $B_{12r}$  occurred at potentials negative to the initial reduction process (see Figures 6 and 7). However, an examination of the magnitude of the absorbance change of both the 525- and 475-nm peaks shows that it is exactly the same as that for the first absorbance waves for the Hg-Ni electrode—no mediator system (see Figures 6 and 7), indicating that even with the mediator the  $B_{12a}$  is only partially reduced at the low negative potentials. The total spectrum of the solution potentiostated at  $-0.6$  V also indicates that part of the  $B_{12a}$  (approximately 35%) is unreacted. The same result was also obtained from the  $n$ -value studies (Table III) at both the Hg-Ni and Au minigrid electrodes. Thus, the unusual two potential processes necessary to totally reduce  $B_{12a}$  appear to be independent of both working electrode material and mediator participation. Neither the spectra for  $B_{12}$  or  $B_{12}$ -CN showed any significant reduction employing Au minigrid-mediator system. No satisfactory mediator with the necessary optical and potential characteristics to explore the  $-0.6$  to  $-1.0$  V potential absorbance behavior at a Hg-Ni minigrid electrode has been found to date.

The half-absorbance potentials for the cobalamin species illustrated in Figures 2 through 9 are presented in Table I.

**Cyclic Voltammetric Behavior of Cobalamins.** Typical cyclic voltammograms of  $B_{12}$  and  $B_{12}$ -CN in a thin layer cell at mercury coated nickel (Hg-Ni) and at Au minigrid electrodes are shown in Figures 10 and 11, respectively. These cyclic voltammograms are quite complex and nonideal with respect to peak shape. The poorly defined waves appear to be caused by both slow electron transfer kinetics and irreversible chemical steps in the redox mechanism associated with each peak. The situation is further complicated by the strong adsorption of both reactants and products.<sup>20</sup> However, based on previous studies<sup>17,20</sup> it is at least qualitatively possible to assign peaks to certain redox processes. Curve A of Figure 10 illustrates the cyclic voltammetric behavior of cyanocobalamin at a Hg-Ni OTTLE. The reduction in the region of  $-0.95$  V corresponds to a two-electron reduction of  $B_{12} + 2e^- \rightarrow B_{12s}[Co(III)] + 2e^- \rightarrow Co(I)]$ .<sup>17-20</sup> Similarly, the anodic peak at  $-0.85$  V on scan reversal is attributable to the process  $B_{12s} - 1e^- \rightarrow B_{12r}[Co(I)] - 1e^- \rightarrow Co(II)]$ .<sup>17-20</sup> An electrochemical study of supporting electrolyte containing a millimolar amount of cyanide has revealed that the anodic peaks in the regions of  $-0.3$  and  $0.0$  V correspond to the redox peaks of the mercury cyanide

**Table I.** Half-Absorbance Potentials<sup>a</sup>

Working electrodes system (OTTLE)	Cobalamin species	Reduction mV vs. SCE	Oxidation mV vs. SCE	Monitored wavelength (nm)
Hg-Ni	B <sub>12</sub> <sup>b,d</sup>	-625 (-875)	-180 (-880)	550
Hg-Ni	B <sub>12</sub> <sup>b,d</sup>	-625 -875	-185 -875	475
Hg-Ni	B <sub>12</sub> -CN <sup>b,c</sup>	-850	-690	580
Hg-Ni	B <sub>12</sub> -CN <sup>b,c</sup>	-825 -910	-689 -910	475
Hg-Ni	B <sub>12a</sub> <sup>b,d</sup>	-60 -635 (-825)	-188 (-825)	530
Hg-Ni	B <sub>12a</sub> <sup>b,d</sup>	-75 -634 -880	-176 -878	475
Au + mediator	B <sub>12</sub> <sup>b,d</sup>	---	---	
Au + mediator	B <sub>12</sub> -CN <sup>b,c</sup>	---	---	
Au + mediator	B <sub>12a</sub> <sup>b,d</sup>	-155	-93	525
Au + mediator	B <sub>12a</sub> <sup>b,d</sup>	-140	-110	475

<sup>a</sup> The cobalamin concentration is 1 mM. It should be pointed out that no relationship between the half-absorbance potentials and the reversible potentials for these species exists at this time.

<sup>b</sup> Supporting electrolyte = 1.0 M Na<sub>2</sub>SO<sub>4</sub>. <sup>c</sup> Supporting electrolyte = 0.1 M KCN. <sup>d</sup> Supporting electrolyte = 0.1 M NaNO<sub>3</sub>.

complex. Mercury cyanide peaks are particularly evident when B<sub>12</sub>-CN was studied, as the supporting electrolyte (1.0 M Na<sub>2</sub>SO<sub>4</sub>) was also 0.1 M in KCN. Though it is not shown on this particular curve (curve A of Figure 10), a cathodic peak does occur in the region of 0.2 V vs. SCE which has been assumed to correspond to B<sub>12r</sub> - 1e<sup>-</sup> → B<sub>12</sub>[Co(II) - 1e<sup>-</sup> → Co(III)].<sup>19,20</sup> Subsequent cycling of B<sub>12</sub> exhibits a new cathodic peak around -0.3 V corresponding to that observed for B<sub>12</sub>-CN and is attributed to the reduction of the mercury cyanide complex.<sup>27,28</sup> Thus, the cyclic voltammogram for B<sub>12</sub>-CN resembles that of B<sub>12</sub> except for the more pronounced mercury cyanide waves.<sup>29,30</sup> The electrochemical behavior of cyano- and dicyanocobalamin at an Au minigrad electrode is shown in Figure 11. The behavior of B<sub>12</sub> and B<sub>12</sub>-CN at an Au minigrad electrode is similar to their behavior at the Hg-Ni minigrad electrode.

When background cyclic voltammograms at the Au OTTLE were run on the supporting electrolyte solution containing millimolar amounts of KCN, no redox peaks were observed. The identity of the peaks in the region from -0.2 to -0.4 V is uncertain and may be evidence of an electron transfer to an adsorbed cobalamin species. These peaks were investigated by potential step methods and will be discussed in the section concerning *n*-value determination.

The cyclic voltammograms for B<sub>12a</sub> at Hg-Ni and Au minigrad electrodes are presented in Figures 12 and 13, respectively. Again it is possible to assign the reduction peak occurring at about -0.95 V to the process B<sub>12a</sub> + 2e<sup>-</sup> → B<sub>12s</sub>[Co(III) + 2e<sup>-</sup> → Co(I)]. The reoxidation peak occurring in the region of -0.8 V appears to correspond to the reaction of B<sub>12s</sub> - 1e<sup>-</sup> → B<sub>12r</sub> while the peak in the region of 0.15 V may correspond to the reaction B<sub>12r</sub> - 1e<sup>-</sup> → B<sub>12a</sub>; similar correlations are possible for the Au minigrad system. Questions now arise as to the identity of the peaks at -0.3 V (oxidation) and 0.2 V (reduction). The reduction peak occurring at 0.2 V is characteristic of the supporting electrolyte (1 M Na<sub>2</sub>SO<sub>4</sub>) Hg-Ni electrode and in some cases is obscured by the cobalamin electrochemistry. The identity of the -0.25 V peak remains uncertain. As the B<sub>12a</sub> was

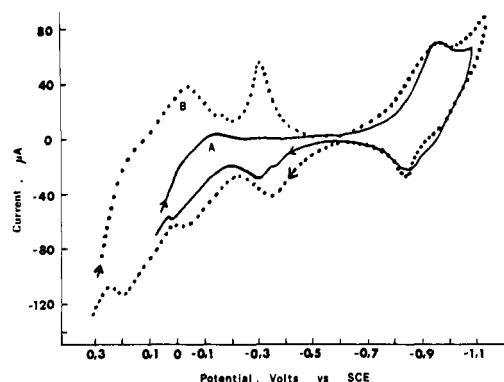


**Figure 10.** Thin layer cyclic voltammograms of 1 mM solutions of cyanocobalamin, B<sub>12</sub> (curve A), and dicyanocobalamin, B<sub>12</sub>-CN (curve B), at the Hg-Ni minigrad electrode: scan rate 2 mV s<sup>-1</sup>; initial scan, negative: (A) B<sub>12</sub>, 1.0 M Na<sub>2</sub>SO<sub>4</sub>, 0.1 M NaNO<sub>3</sub>, pH 7.0; (B) B<sub>12</sub>-CN, 1.0 M Na<sub>2</sub>SO<sub>4</sub>, 0.1 M KCN, pH 10.4.

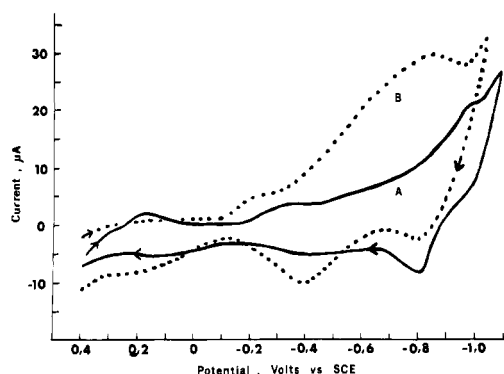


**Figure 11.** Thin layer cyclic voltammogram of 1 mM solutions of B<sub>12</sub> (curve A) and B<sub>12</sub>-CN (curve B) at the Au minigrad electrode: scan rate 2 mV s<sup>-1</sup>; initial scan, negative: (A) B<sub>12</sub>, 1.0 M Na<sub>2</sub>SO<sub>4</sub>, 0.1 M NaNO<sub>3</sub>, pH 7.0; (B) B<sub>12</sub>-CN, 1.0 M Na<sub>2</sub>SO<sub>4</sub>, 0.1 M KCN, pH 10.4.

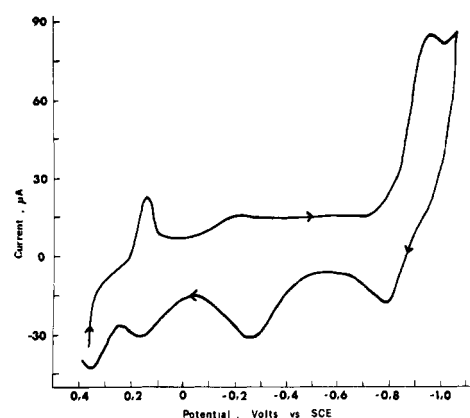


**Figure 12.** Thin layer cyclic voltammograms of 0.9 mM solutions of aquocobalamin, B<sub>12a</sub>, at the Hg-Ni minigrad electrode: 1.0 M Na<sub>2</sub>SO<sub>4</sub>; 0.1 M NaNO<sub>3</sub>; pH is 7.0; scan rate 2 mV s<sup>-1</sup>; initial scan, negative.

synthesized from B<sub>12</sub> itself, the first inclination is to attribute this anodic peak to the formation of a mercury(II) cyanide complex as the potential range is similar to that observed in Figure 10 for mercury(II) cyanide formation. The cyanide would come from unconverted B<sub>12</sub> starting material if the synthesis was incomplete. However, for a number of reasons discussed below no cyanide is thought to be present in the B<sub>12a</sub> solutions. On a repeated scan of the B<sub>12a</sub> solution the mercury cyanide reduction peak is not observed. Furthermore, B<sub>12a</sub> samples prepared by various other routes

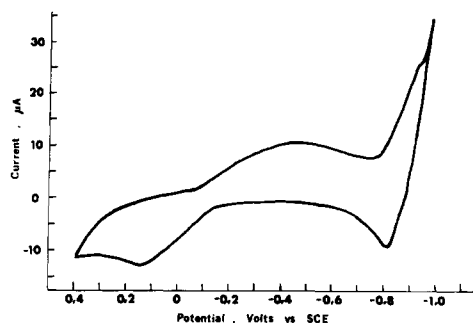


**Figure 13.** Thin layer cyclic voltammograms of 0.9 mM solutions of aquocobalamin, B<sub>12a</sub>, at the Au minigrid electrode: 1.0 M Na<sub>2</sub>SO<sub>4</sub>; 0.1 M NaNO<sub>3</sub>; pH is 7.0; scan rate 2 mV s<sup>-1</sup>; initial scan, negative.

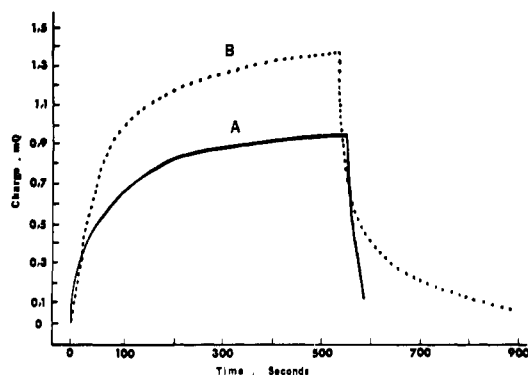


**Figure 14.** Charge-time curve for the application of a potential step from 0.000 to -0.970 to +0.100 V vs. SCE at a Hg-Ni OTTLE: (A) background, 1.0 M Na<sub>2</sub>SO<sub>4</sub>, 0.1 M NaNO<sub>3</sub>; (B) B<sub>12</sub>, 0.6 mM B<sub>12</sub>, 1.0 M Na<sub>2</sub>SO<sub>4</sub>, 0.1 M NaNO<sub>3</sub>.

(chemical, electrochemical, and microbial syntheses, as described in the experimental section) were studied, and in all cases the peak at about -0.25 V was present. It seems unlikely that a common cyanide impurity of the same concentration would be present in the diversely prepared samples. Also, cyclic voltammograms were obtained for the B<sub>12a</sub> at a HMDE (hanging mercury drop electrode) with no indication of any peak in the region -0.25 to 0.3 V. This leads one to speculate that perhaps this -0.25 V unique redox process may be occurring between the base-off cob(I) or cob(II)alamin species and the Hg-Ni surface. Such an interaction for base-off cobalamins, with transition metals and transition metal complexes, is well documented in the literature.<sup>31</sup>

***n*-Value Determination.** Controlled potential coulometry with a thin layer minigrid electrode system<sup>22,23</sup> was used to determine the number of electrons (*n*-value) for various waves found in the cyclic voltammograms of each of the cobalamins. A typical charge vs. time curve for B<sub>12</sub> is shown in Figure 14. It was necessary to extrapolate the final sloping portion of the *Q*-*t* curve back to *t* = 0 to correct for edge effects inherent in the thin layer cell system.<sup>32</sup> The method for correction and calculation of *n*-values for charging and residual current by repeating the experiment on the supporting electrolyte has been described previously.<sup>23</sup> The *n* values, as well as the initial and final values of the applied potential steps, are shown in Table II. For the three cob(III)alamin systems using the Hg-Ni minigrid electrode, only one reduction wave is observed in the -1.0 V vs. SCE potential region (see Figures 10 through 13) and the *n* value obtained in each case from the *Q* vs. *t* data was effectively two (2) yielding a cob(I)alamin product in each case which confirms polarographic and other previously reported results.<sup>2-20</sup> As expected, the background breakdown potential

**Table II.** *n*-Value Results

Minigrid working electrode system	Potential step region mV vs. SCE	Species	No. of electrons = <i>n</i>
<b>Reduction Coulometry</b>			
Hg-Ni	0 to -970	B <sub>12</sub> <sup>a,c</sup>	1.90
		B <sub>12</sub> -CN <sup>a,b</sup>	2.00
		B <sub>12a</sub> <sup>a,c</sup>	1.96
Au	0 to -500	B <sub>12</sub> <sup>a,c</sup>	0.013
	+300 to -400	B <sub>12</sub> -CN <sup>a,b</sup>	0.126
	+100 to -1000	B <sub>12</sub> -CN <sup>a,b</sup>	1.37
	+300 to -600	B <sub>12a</sub> <sup>a,c</sup>	0.65
<b>Oxidation Coulometry</b>			
Hg-Ni	-970 to +100	B <sub>12</sub> <sup>a,c</sup>	2.14
		B <sub>12</sub> -CN <sup>a,b</sup>	0.51
		B <sub>12a</sub>	0.38
Au	-500 to 0	B <sub>12</sub> <sup>a,c</sup>	0.013
	-400 to +300	B <sub>12</sub> -CN <sup>a,b</sup>	0.125
	-1000 to +100	B <sub>12</sub> -CN <sup>a,b</sup>	1.40
	-600 to +300	B <sub>12a</sub> <sup>a,c</sup>	0.65

<sup>a</sup> Supporting electrolyte = 1.0 M Na<sub>2</sub>SO<sub>4</sub>. <sup>b</sup> Supporting electrolyte = 0.1 M KCN. <sup>c</sup> Supporting electrolyte = 0.1 M NaNO<sub>3</sub>. The cobalamin concentration is 1 mM.

shifts positive on the Au minigrid electrode and overlaps the Co(III)-Co(I) wave observed on the Hg-Ni electrode. On Au electrodes, B<sub>12</sub> and B<sub>12</sub>-CN exhibit a small prewave at -0.3 V and a broad irreversible appearing wave at about -0.8 V. The B<sub>12a</sub> exhibits a single very broad poorly defined wave with a peak potential at about -0.5 V. Potential step experiments with B<sub>12</sub>-CN gave fractional *n* values regardless of the magnitude of the first applied potential, the meaning of which could not be interpreted from the electrochemical data. The *n* value for B<sub>12a</sub> on a potential step to -0.6 V also yielded a fractional value of about 0.65. It has been previously reported by some workers that only B<sub>12a</sub> can be coulometrically reduced to B<sub>12</sub>, (cob(II)alamin) in a one-electron step at a mercury electrode at intermediate potentials.<sup>6,11</sup> At a Hg-Ni minigrid, the three cob(III)alamins were coulometrically reduced to cob(I)alamin at -0.97 V and the potential was stepped to +0.1 V and the *Q* vs. *t* curves were recorded. Only in the B<sub>12</sub> case was a reoxidation *n* value equal to 2 found which indicates a virtually quantitative reoxidation to B<sub>12</sub>. Fractional *n* values obtained for B<sub>12a</sub> and B<sub>12</sub>-CN derived cob(I)alamins indicates that only part of these cob(III)alamins are regenerated even at positive potentials. However, these reoxidation *n* values are difficult to interpret as complicating effects arise from the interfering mercury(II) cyanide species which form in some cases.<sup>26,27</sup> At the Au minigrid electrodes only part of the cob(III)alamins are reduced as explained above; however, it appears from the reoxidation *n* values that the fraction reduced is quantitatively regenerated at positive potentials. The ability of the base-off cobalamin to form complexes with metal ions also obscures the issue.<sup>30</sup>

Further *n*-value information was obtained by fixed wavelength optical monitoring techniques coupled with controlled potential coulometry to determine *n* values for appropriate redox processes involving vitamin B<sub>12</sub>. As mentioned previously B<sub>12</sub> was chosen for this investigation as earlier studies had suggested that B<sub>12</sub> underwent only a single two-electron reduction step.<sup>2-14</sup> The monitoring wavelength of 475 nm was chosen as this peak is indicative of the presence (or absence) of a cob(II)alamin. Monitoring this wavelength, while coulometrically the number of electrons transferred to the cobalamin in the process is measured,

**Table III.** Spectropotential Step  $n$ -Values for B<sub>12</sub>

Working electrode system (OTTLE)	Potential step V vs. SCE		Monitored wavelength (nm)	No. of electrons
	From	To		
Hg-Ni	Rest	-0.755	475	0.98
	-0.755	0.200	475	<i>a</i>
	Rest	-0.755	475	0.99
	-0.755	-1.000	475	0.93
	-1.000	-0.755	475	1.04
	-0.755	0.200	475	<i>a</i>

<sup>a</sup> Catalytic process,  $n > 2$ .

yields the  $n$  value for each step of the mechanism. Table III summarizes the results of this spectroelectrochemical study. It is evident from the growth and decay of the 475-nm peak that a one-electron reduction does occur at intermediate potentials and that this species can undergo a further one-electron transfer to form cob(I)alamin. The  $n$  value in this case cannot be determined directly because of interference from background. This cob(I)alamin is readily reoxidized to a cob(II)alamin;  $n$  value equals one. Existing experimental conditions again did not allow for an accurate determination of the  $n$  value for the reoxidation to a cob(III)alamin.

### Conclusions

The results described above show that, in spite of the fact that the electrokinetic data are very complicated, unusual, and virtually impossible to interpret mechanistically, the optical monitoring of the solution composition using the OTTLE technique gives a good picture of the net or overall redox reactions that take place.

The first observation of significance is that all three cob(III)alamins (B<sub>12</sub>, B<sub>12</sub>-CN, and B<sub>12a</sub>) undergo a quantitative one-electron reduction to either the same or similar cob(II)alamin (B<sub>12r</sub>) species at intermediate potentials in the 0.0 to -0.8 V range. Previous electrochemical studies by other groups had claimed that only B<sub>12a</sub> could be reduced to B<sub>12r</sub> at intermediate potentials.<sup>6,11</sup> As the polarographic and cyclic voltammetric studies did not indicate any discernible waves in this potential range for B<sub>12</sub> or B<sub>12</sub>-CN, it appears that no one had, therefore, attempted coulometric reductions at such potentials. However, the OTTLE results clearly show that the one-electron reaction is common to all the species but that in the case of B<sub>12</sub> and B<sub>12</sub>-CN the kinetics of the reaction is unusually slow even with respect to the slow scan rates employed in polarography and the cyclic voltammetry reported here. These one-electron processes for B<sub>12</sub> and B<sub>12</sub>-CN show up only during point-by-point potentiostatic OTTLE techniques. The reason for the extremely slow kinetics of this one-electron reaction has not been elucidated at this time. The electron transfer rate is fast enough for waves to be observed polarographically or with cyclic voltammetry only in the B<sub>12a</sub> case. Under the same conditions the further reduction of all the cobalamin systems from the Co(II) to Co(I) oxidation state was quantitative and "reversible". The apparent hysteresis involving Co(II) to Co(III) cobalamins is not presently well understood but may result from chemical reactions involved in the mechanism.

It is interesting to note that B<sub>12</sub>-CN is totally re-formed (shown in curve B, Figure 5) while cyanocob(I)alamin does not completely reoxidize to B<sub>12</sub>. This suggests that B<sub>12</sub> and B<sub>12</sub>-CN may reoxidize by separate pathways. Because of the magnitude of the irreversibility of the B<sub>12</sub> redox couple and also the fact that B<sub>12</sub> is not totally re-formed (some

B<sub>12a</sub> appears to be a minor reoxidation product), it is thought that on electrochemical reoxidation that B<sub>12a</sub> is the initial product formed and that B<sub>12</sub> subsequently forms on a ligand exchange reaction involving the cyanide in solution (initially released into the solution phase during the reduction of B<sub>12</sub> to B<sub>12r</sub>, as shown by the fact that a -0.1 to -0.8 V OTTLE experiment (cob(III)alamin ↔ cob(II)alamin) with vitamin B<sub>12</sub> shows the same large irreversibility indicating that the CN<sup>-</sup> is lost in the first reduction step). This ligand exchange reaction of B<sub>12a</sub> with CN<sup>-</sup> has been shown to be very fast.<sup>33</sup> However, the net rate is slow because of the dilute solutions employed. The complete regeneration of B<sub>12</sub> is not possible as some CN<sup>-</sup> is lost, probably through the formation of stable mercury(II) cyanide complexes.<sup>27-29</sup> It was noted that the percent recovery increased on addition of excess cyanide which is consistent with this interpretation. With respect to B<sub>12</sub>-CN, the final product is formed directly upon reoxidation or the follow-up ligand exchange reaction between the concentrated cyanide solution and the B<sub>12a</sub>, formed by the loss of one electron from B<sub>12r</sub> (with water molecules in the axial positions<sup>34</sup>), is very fast.

At this time it is impossible to distinguish between these two mechanisms for the reoxidation of B<sub>12</sub>-CN. However, it should be noted that the B<sub>12r</sub> spectra (as indicated by the 475-nm peak) in both B<sub>12</sub> and B<sub>12</sub>-CN reactions are virtually identical.

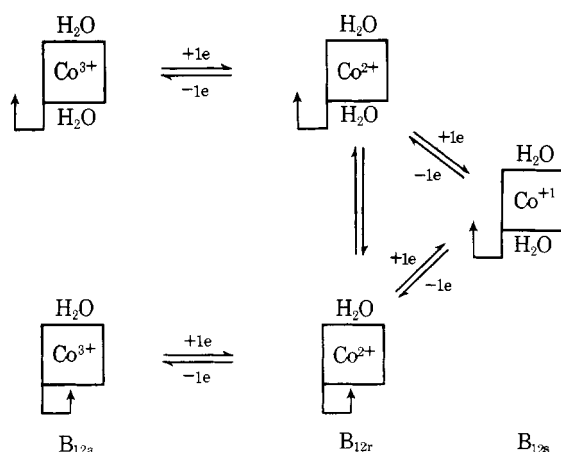
Perhaps the most unusual and difficult to understand result is the observation of two different potential-absorbance "waves" for the reduction of B<sub>12a</sub> to a cob(II)alamin. The OTTLE spectra and the apparent  $n$ -value data indicate that B<sub>12a</sub> converts to B<sub>12r</sub> (about 65%) at potentials around -0.05 V at both the Hg-Ni and Au electrodes while it is necessary to raise the potential to greater than -0.6 V where the second wave corresponding to the reduction of the remaining 35% of the B<sub>12a</sub> is observed. The most obvious conclusion that fits the data qualitatively is that the B<sub>12a</sub> employed in these experiments was impure and contained about 35% of B<sub>12</sub> itself (B<sub>12a</sub> was prepared from B<sub>12</sub>).<sup>13</sup> However, as pointed out above, we found that *all* batches of B<sub>12a</sub> gave the same results which again would not be expected to remain constant if the various synthesis routes yielded only partial conversion. Also the spectral and polarographic properties do not suggest that any appreciable concentration of B<sub>12</sub> remain unconverted and also are identical with the spectra and polarographic properties of vitamin B<sub>12a</sub> produced by the totally different procedures.

Furthermore, there is considerable other indirect evidence that there is no significant unconverted B<sub>12</sub> in the B<sub>12a</sub> samples. Note first of all that there is no -0.6 V polarographic wave for B<sub>12</sub> that corresponds to the wave for this second B<sub>12a</sub> species. (It is interesting to note that previous polarographic studies had referred to the wave at -0.6 V as an impurity.)<sup>11,35</sup> Although the cyclic voltammogram for B<sub>12a</sub> shown in Figure 12 does exhibit an anodic peak at -0.28 V which could be indicative of Hg oxidation in the presence of a complexing ligand, this wave is about 50 mV positive to the peak corresponding to mercury-cyanide formation in the B<sub>12</sub> cyclic voltammogram and there is no corresponding mercury cyanide reduction peak on a subsequent cathodic sweep of B<sub>12a</sub> as is *always* the case for subsequent cathodic sweeps of B<sub>12</sub> itself. Finally high pressure liquid chromatography (using a mixture of either 80% isopropyl alcohol and 20% water, or 65% methanol and 35% water, at 2000 psi on an Aminex A-4 column, with detector wavelength set at  $\lambda$  360 nm) on B<sub>12a</sub> has exhibited two closely spaced yet distinct peaks both with retention times that are different than B<sub>12</sub>. Also, a thin layer chromatographic comparison of B<sub>12</sub> and B<sub>12a</sub> using a 65% methanol and 35% water solvent system has shown that B<sub>12</sub> and B<sub>12a</sub>



have relative fronts, though no separation of  $B_{12a}$  itself was observed. It is felt that ring structure differences would not account for the two unique  $B_{12a}$  species, as the  $B_{12a}$  prepared from three techniques (potentiostatic, biological and chemical) would not give identical 65/35 ratio of concentrations. Moreover, it is hard to understand how two different rings, which would be expected to be common to all cobalamins, exhibit drastic reduction potential differences for  $B_{12a}$  and not for  $B_{12}$  or  $B_{12}$ -CN. Thus, it is attractive to speculate that the two species represent differences in axial ligand configuration. The simplest answer would be that one of the  $B_{12a}$  species contains water molecules in the X and Y positions (the "base-off" form) while the other is in the configuration with one water in the X position and the 5,6-dimethylbenzimidazole in the Y position (the "base-on" form). The spectroelectrochemical data clearly demonstrate that the two  $B_{12a}$  species are not in equilibrium. However, Thusius has shown that the X position of  $B_{12a}$  is very labile (rate constants of about  $170\text{--}2300\text{ M s}^{-1}$ ).<sup>32</sup> However, no measurements have been made on the Y-position benzimidazole- $H_2O$  exchange rates.<sup>36</sup> It is possible that this exchange could be very slow. The fact that the diaquocob(III)inamide (having no benzimidazole attached to the corrin ring side chain) is difficult to reduce ( $E_{1/2} \approx -0.7\text{ V}$ )<sup>36</sup> is consistent but not proof of the "base-on"-"base-off" explanation. This fact suggests that the "base-on" aquocob(III)alamin form has a configuration favorable to reduction (the  $-0.15\text{ V}$  wave) and the "base-off" form which would closely correspond to a diaquocob(III)inamide configuration is difficult to reduce ( $-0.6\text{ V}$  wave).<sup>36</sup> The cob(III)alamin reduction product,  $B_{12r}$ , has already been shown to exist as two forms (also speculated to be "base on" and "base off" forms) in a previous study on the oxidation of cob(I)alamins.<sup>37</sup> This cob(II)alamin would be expected to exist at equilibrium in the time frame of the OTTLE experiment as Co(II) species are generally labile.<sup>38</sup> If this equilibrium is rapid, one would anticipate a single reoxidation absorbance-potential wave which is observed. However, it would be expected that the absorbance half-wave potential would occur at the  $-0.6\text{ V}$  range where the difficult to reduce and hence more easily oxidized form would lose an electron. The reoxidation occurs at  $-0.15\text{ V}$  and it was found that all subsequent OTTLE reductions still exhibited the same 65/35 ratio of the two  $B_{12a}$  forms. Thus, one is forced to argue from the OTTLE data that the equilibrium between the two  $B_{12r}$  forms is *slow* compared to the oxidation electron transfer rates and that the oxidation potentials of the two  $B_{12r}$  species are identical. Hence, on oxidation the two  $B_{12r}$  species are trapped as the two inert  $B_{12a}$  forms. Based on this reasoning, it is speculated that the qualitative reaction sequence for the redox mechanism of

Scheme I



the aquocobalamin system follows the path indicated in Scheme I.

The cob(II)alamin-cob(I)alamin redox mechanism was observed to be reversible with respect to the potentiostatic OTTLE experiment. Thus, if two  $B_{12r}$  species exist, they either have the same reduction potential or the homogeneous equilibrium must be relatively *fast* compared to the reduction electron transfer rates. Thus the interpretation of the redox and equilibrium behavior of  $B_{12r}$  and  $B_{12r}'$  using a "base-on" and "base-off" model appears *contradictory*. However, as no diffusion model has been devised for the OTTLE system, it is impossible to make any studies of kinetic parameters at this time.

It is obvious that there are many unanswered questions concerning rates of the microscopic processes involved in the redox chemistry of cobalamin complexes. However, the macroscopic resultant effect of electrode potential on solution composition is now well defined. With this basic overall mechanistic information, a more comprehensive study of the electrode kinetics and time resolved spectral studies on potential step experiments on these and other cobalamins under variable conditions of pH, supporting electrolyte, and electrode material may elucidate all the steps in the overall mechanism.

**Acknowledgments.** The authors gratefully acknowledge financial assistance received through National Science Foundation Grants GP-35979 (H.B.M.) and GP-41981X (W.R.H.), and through a Cottrell Grant from Research Corporation (H.B.M.) for the purchase of a high pressure liquid chromatograph. We gratefully acknowledge Dr. E. A. Deutsch for helpful discussions and for the use of alternate  $B_{12a}$  samples and thank Robert J. Nowak and Mark S. Denton for performing the cobalamin chromatographic separations.

## References and Notes

- (1) F. M. Huennekense in "Biological Oxidations", T. P. Singer, Ed., Interscience, New York, N.Y., 1968, pp 482-502.
- (2) H. Diehl, R. R. Sealock, and J. Morrison, *Iowa State Coll. J. Sci.*, **24**, 433 (1950).
- (3) H. Diehl, J. I. Morrison, and R. R. Sealock, *Experientia*, **7**, 60 (1951).
- (4) H. Diehl, and J. I. Morrison, *Rec. Chem. Prog.*, **31**, 15 (1952).
- (5) R. N. Boos, J. E. Carr, and J. B. Conn, *Science*, **117**, 603 (1953).
- (6) B. Jaselskis and H. Diehl, *J. Am. Chem. Soc.*, **81**, 4345 (1959).
- (7) B. Jaselskis and H. Diehl, *J. Am. Chem. Soc.*, **80**, 2147 (1958).
- (8) J. W. Collat and S. L. Tackett, *J. Electroanal. Chem.*, **4**, 59 (1962).
- (9) S. L. Tackett, Ph.D. Thesis, Ohio State University, 1962.
- (10) B. Kratochvil and H. Diehl, *Talanta*, **13**, 1013 (1966).
- (11) H. P. C. Hogenkamp and S. Holmes, *Biochemistry*, **9**, 1888 (1970).
- (12) D. Lexa and J. M. L'hoste in "Biological Aspects of Electrochemistry", G. Milazzo, P. E. Jones, and L. Rampazzo, Ed., Birkhauser Verlag, Stuttgart, 1971, pp 395-404.
- (13) T. M. Kenyhercz and H. B. Mark, Jr., *Anal. Lett.*, **7**, 1 (1974).
- (14) B. A. Abd-el-Nabey, *J. Electroanal. Chem.*, **53**, 17 (1974).
- (15) S. L. Tackett, J. W. Collat, and J. C. Abbott, *Biochemistry*, **2**, 919 (1963).
- (16) P. K. Das et al., *Biochim. Biophys. Acta*, **141**, 644 (1967).
- (17) S. L. Tackett and J. W. Ide, *J. Electroanal. Chem.*, **30**, 510 (1971).
- (18) P. G. Swetik and D. G. Brown, *J. Electroanal. Chem.*, **51**, 433 (1974).
- (19) R. L. Birke, G. A. Brydon, and M. F. Boyle, *J. Electroanal. Chem.*, **52**, 237 (1974).
- (20) T. M. Kenyhercz and H. B. Mark, Jr., in preparation to be submitted to this journal.
- (21) R. W. Murray, W. R. Heineman, and G. W. O'Dom, *Anal. Chem.*, **39**, 1866 (1967).
- (22) W. R. Heineman, B. J. Norris, and J. F. Goelz, *Anal. Chem.*, **47**, 79 (1975).
- (23) W. R. Heineman, T. P. DeAngelis, and J. F. Goelz, *Anal. Chem.*, **47**, 1364 (1975).
- (24) Provided by Dr. E. A. Deutsch, Department of Chemistry, University of Cincinnati.
- (25) G. H. Beaven and E. A. Johnson, *Nature (London)*, **176**, 1264 (1955).
- (26) It should be pointed out the reaction  $B_{12a} \rightleftharpoons [H^+] + B_{12b}$  (hydroxycob(III)alamin) has a  $pK_a$  of 7.8 and a more negative reduction potential than  $B_{12a}$ ; H. O. A. Hill, "Inorganic Biochemistry", Vol. 2, G. Eichcon, Ed., Elsevier, New York, N.Y., 1973, Chapter 30. This proton equilibrium is undoubtedly fast and, thus, only the reduction of the  $B_{12a}$  will be observed in these OTTLE experiments.
- (27) T. Sekine, Y. Komatsu, and J. Yumikura, *J. Inorg. Nucl. Chem.*, **35**, 3891 (1973).



- (28) J. Heyrovsky and J. Kuta, "Principles of Polarography", Academic Press, New York, N.Y., 1966, p 168.  
 (29) Reference 28, pp 175–176.  
 (30) F. A. Cotton and G. Wilkinson, "Advanced Inorganic Chemistry", 3d ed, Interscience, New York, N.Y., 1972, p 519.  
 (31) (a) J. M. Pratt, "Inorganic Chemistry of Vitamin B<sub>12</sub>", Academic Press, New York, N.Y., 1972, p 162; (b) W. M. Scovell, *J. Am. Chem. Soc.*, **96**, 3451 (1974), and references therein.  
 (32) B. McDuffie, L. B. Anderson and C. N. Reilley, *Anal. Chem.*, **38**, 883 (1966).  
 (33) D. Thusius, *J. Am. Chem. Soc.*, **93**, 2629 (1971).  
 (34) T. M. Kenyhercz, A. M. Yacynych, and H. B. Mark, Jr., submitted to *J. Am. Chem. Soc.*  
 (35) Reference 6, p 4346.  
 (36) Reference 11, p 1889.  
 (37) T. M. Kenyhercz, A. M. Yacynych, and H. B. Mark, Jr., submitted to *J. Am. Chem. Soc.*  
 (38) F. Basolo and R. G. Pearson, "Mechanisms of Inorganic Reactions A Study of Metal Complexes in Solution", 2d ed, Wiley, New York, N.Y., 1967, p 144.

## Preparation and Spectroscopic Properties of Cobalt(III) Complexes Containing Phosphine Ligands. The Electronic Structural Description of Side-Bonded Dioxygen

Vincent M. Miskowski, John L. Robbins, George S. Hammond, and Harry B. Gray\*

Contribution No. 4983 from the Arthur Amos Noyes Laboratory of Chemical Physics, California Institute of Technology, Pasadena, California 91125.

Received August 4, 1975

**Abstract:** The cobalt(III) complexes  $[\text{Co}(\text{2=phos})_2\text{X}_2]\text{ClO}_4$  ( $\text{X}^- = \text{Cl}^-, \text{Br}^-, \text{NCO}^-, \text{N}_3^-, \text{NCS}^-$ ), where 2=phos is *cis*-1,2-bis(diphenylphosphino)ethylene, have been prepared. The infrared and electronic spectral properties of these complexes are consistent with an assignment of *trans* stereochemistry. The corresponding cobalt(III) complexes of 2—phos (1,2-bis(diphenylphosphino)ethane) are extremely unstable. Furthermore, several reactions of the  $[\text{Co}(\text{2=phos})_2\text{X}_2]^+$  complexes give unexpected products; thus, reaction with  $\text{NO}_2^-$  yields  $[\text{Co}(\text{2=phos})(\text{NO})_2]^+$ . Variations in the stabilities of the complexes of 2=phos and 2—phos apparently are related to differences in nonbonding interactions of phenyl groups with the axial ligands. Special attention has been paid to the formulation of the electronic structures of  $[\text{Co}(\text{2=phos})_2\text{O}_2]^+$  and related rhodium and iridium complexes. The  $\text{PF}_6^-$  salt of  $[\text{Co}(\text{2=phos})_2\text{O}_2]^+$  exhibits electronic absorption bands at 21.6 ( $\epsilon$  1170), 26 ( $\epsilon$  1200), and 31.4 ( $\epsilon$  24 500) kK at 77 K in a 12:1 EPA- $\text{CHCl}_3$  glass. As the spectrum is strikingly similar to that of the analogous Co(III)-carbonato complex,  $[\text{Co}(\text{2=phos})_2\text{CO}_3]^+$ , assignment of the 21.6 and 26 kK bands to the two spin-allowed d-d transitions ( $^1\text{A}_1 \rightarrow ^1\text{T}_1$ ,  $^1\text{T}_2$ ) expected for a  $[\text{Co}^{\text{III}}\text{P}_4(\text{O}_2^{2-})]^+$  ground state is indicated. The intense band at 31.4 kK is attributed to an allowed  $\sigma(\text{P}) \rightarrow d\sigma^*(\text{Co})$  charge transfer transition. The electronic spectrum of  $[\text{Ir}(\text{2=phos})_2\text{O}_2]^+$  is also reported. The lowest energy feature, a broad shoulder in the 33–34-kK region, is attributed to  $^1\text{A}_1 \rightarrow ^1\text{T}_1$  in an  $[\text{Ir}^{\text{III}}\text{P}_4(\text{O}_2^{2-})]^+$  center.

In 1963, Vaska reported that *trans*- $[\text{Ir}(\text{PPh}_3)_2(\text{CO})\text{Cl}]$  reacts reversibly with dioxygen to give a 1:1 adduct complex.<sup>1</sup> The subsequent crystal structure determination showed the dioxygen to be side-bonded to the metal, the  $\text{IrO}_2$  unit forming an isosceles triangle.<sup>2</sup> Similar dioxygen adducts have since been prepared with many other central metal ions.<sup>3–5</sup> Although the formation of such adducts is generally thought to involve oxidation of the central metal,<sup>5</sup> little detailed electronic structural information is available that bears on the point. For example, there have been very few attempts to analyze in any depth the electronic spectra of side-bonded dioxygen complexes.

The investigations outlined in this paper were prompted by the report<sup>6</sup> of a side-bonded dioxygen adduct of  $[\text{Co}(\text{2=phos})_2]^+$ , where 2=phos is *cis*-1,2-bis(diphenylphosphino)ethylene. We have found that it is possible to prepare an extensive series of complexes of the type  $[\text{Co}(\text{2=phos})_2\text{X}_2]^+$ , whereas all the 2—phos (1,2-bis(diphenylphosphino)ethane) analogues appear to be unstable. The chemistry of these 2=phos complexes has proved to include some surprising redox instability patterns, which we have attempted to analyze. We also have interpreted the electronic spectroscopic properties of  $[\text{Co}(\text{2=phos})_2\text{X}_2]^+$  by reference to other Co(III) complexes and to Rh(III) analogues. The spectrum of  $[\text{Co}(\text{2=phos})_2\text{O}_2]^+$  has been examined with particular care, as it contains information about the electronic structure of the  $\text{CoO}_2^+$  unit. In addition, we have attempted to correlate the electronic spectro-

scopic properties of  $[\text{Co}(\text{2=phos})_2\text{O}_2]^+$  with those of the corresponding rhodium and iridium complexes.

### Experimental Section

The phosphine ligands were obtained from Pressure Chemical Co. and were used as received. All other reagents and solvents were at least analytical reagent grade. The compounds  $\text{Co}(\text{2—phos})_2\text{X}_2$  ( $\text{X}^- = \text{Cl}^-, \text{Br}^-$ ) were prepared by the method of Horrocks et al.<sup>7</sup> The compounds  $\text{Co}(\text{2=phos})_2\text{X}_2 \cdot \text{CoX}_2$  ( $\text{X}^- = \text{Cl}^-, \text{Br}^-, \text{I}^-$ ) were prepared by the same procedure. The formulation given for the latter complexes is based on elemental analyses, which, assuming the stoichiometry  $\text{Co}(\text{2=phos})_2\text{X}_2 \cdot n\text{CoX}_2$ , consistently gave  $n = 0.9\text{--}1.2$ . (Example analysis: Calcd for  $\text{Co}(\text{2=phos})_2\text{Cl}_2 \cdot \text{CoCl}_2$ : C, 59.34; H, 4.22; Cl, 13.47; Co, 11.2. Found: C, 58.67; H, 3.69; Cl, 13.11; Co, 12.9.) The compounds presumably are  $[\text{Co}_2\text{X}_6]^{2-}$  salts of  $[\text{Co}(\text{2=phos})_2\text{X}]^+$ .

**$[\text{Co}(\text{2=phos})_2](\text{ClO}_4)_2$ .** A solution of 0.75 g of  $\text{Co}(\text{ClO}_4)_2 \cdot 6\text{H}_2\text{O}$  in 15 ml of acetone was added under nitrogen to a solution of 0.65 g of 2=phos in 30 ml of acetone. The solution turned orange, and a yellow product began to form. After storage at 10° for 1 h, the solution was filtered under nitrogen. The bright-yellow crystalline product was washed with methanol and ether. It is indefinitely stable in air when dry. Anal. Calcd for  $[\text{Co}(\text{2=phos})_2](\text{ClO}_4)_2$ : C, 59.22; H, 4.59; P, 11.75. Found: C, 58.62; H, 4.28; P, 11.72.

**$[\text{Co}(\text{2=phos})_2](\text{BF}_4)_2$**  was prepared similarly, from  $\text{Co}(\text{BF}_4)_2 \cdot 6\text{H}_2\text{O}$ , and obtained as yellow crystals. Anal. Calcd for  $[\text{Co}(\text{2=phos})_2](\text{BF}_4)_2$ : C, 60.91; H, 4.33. Found: C, 60.81; H, 4.33.

**$[\text{Co}(\text{2=phos})_2\text{Cl}_2]\text{ClO}_4$ .** Chlorine gas was bubbled through a solution of  $\text{Co}(\text{2=phos})_2\text{Cl}_2 \cdot \text{CoCl}_2$  (0.5 g) in 25 ml of  $\text{CH}_2\text{Cl}_2$ , in the dark. A green solid began to form almost immediately. After 15 min, the solution was flushed with nitrogen briefly to remove